MiR-323a-3p Inhibits Tumor Growth and Gefitinib Resistance Acquisition by Targeting EGFR/ErbB3 in Colorectal Cancer

Yuanzhou Zhang
Shanghai Cancer Institute
Shunshun Liang
Shanghai Cancer Institute
Bowen Xiao
Shanghai Cancer Institute
Jingying Hu
Shanghai Cancer Institute
Yechun Pang
Shanghai Cancer Institute
Yuling Liu
Shanghai Cancer Institute
Juan Yang
Shanghai Cancer Institute
Junpin Ao
Shanghai Cancer Institute
Lin Wei
Shanghai Cancer Institute
Xiaoying Luo (luoxy@shsci.org)
Shanghai Jiao Tong University School of Medicine

Research Article

Keywords: Kras mutant, colorectal cancer, ErbB3, miR-323a-3p, EGFR-TKI resistance

Posted Date: June 8th, 2021

DOI: https://doi.org/10.21203/rs.3.rs-571141/v1

Abstract

Background: EGFR-TKIs are prone to develop acquired drug resistance in colorectal cancer and are only applicable in Kras wild type colorectal cancer patients. This study aimed to determine the reasons for the poor treatment efficacy of TKIs in Kras mutant CRC and to improve the treatment effect.

Method: The RTK Phosphorylation Membrane array was used to detect and screen changes in phosphorylated protein levels in KRAS mutant-resistant CRC cells. qRT-PCR, western blot and TCGA database were applied for reporting the expression of ERGR and ErbB3 in CRC. Luciferase reporter and western blot examined the network of miR-323a-3p. RTCA, colony formation, CCK-8, caspase-3/7 activity and Flow cytometry probed the impacts of miR-323a-3p on CRC cell growth.

Results: We illustrated that ErbB3 and EGFR were activated in gefitinib-resistant Kras mutant colorectal cancer cell lines. ErbB3 is highly expressed in Kras mutant patient tissues, and patients with $ErbB3^{high}/EGFR^{high}$ had a poorer prognosis. Mechanically, We found and verified that the tumor suppressor miR-323a-3p simultaneously directly targeted EGFR/ErbB3 and inhibited tumor cell growth by activating the apoptosis pathway. Further functionality studies identified miR-323a-3p synergized with gefitinib to inhibit tumor growth, and this synergy prevented the development of acquired resistance to gefitinib in CRC cell lines.

Conclusion: Accordingly, these data indicate that Kras mutant CRC TKI resistance occurs due to the activation of EGFR and ErbB3. Thus, miR-323a-3p has the potential to treat Kras-mutated colorectal cancer by targeting ErbB3/EGFR.

Background

Colorectal cancer (CRC) is the second leading cause of cancer-related death worldwide (1–3). The numbers of new cases of colorectal cancer in developed countries are 6 times higher than those in developing countries, while the mortality rate is the same (2). Although screening and excision of precancerous lesions have reduced the mortality of early CRC (4), the overall survival rate is still low due to late CRC metastasis and chemotherapy resistance (5).

In clinical practice, EGFR-targeted therapy can improve the overall survival (OS) in Kras wild type colorectal cancer patients (6), which is an important method of targeted therapy for colorectal cancer patients. However, multiple factors, such as APC, Kras, TP53, BRAF, PIK3CA (7, 8) and other gene mutations leading to the heterogeneity of CRC cells, limit the therapeutic efficacy of single-targeting EGFR in CRC. Kras gene mutations are a major factor in colorectal cancer. Furthermore, data show that the probability of Kras gene mutations in Chinese colorectal cancer patients is as high as 30%-50%; likewise, Kras gene mutations are a key factor leading to tumor metastasis, recurrence and drug resistance (9).

Nevertheless, recent studies have reported that Kras mutant lung adenocarcinoma resistance to first-generation tyrosine kinase inhibitors (TKIs) is not due to downstream Kras activation but rather to

activation of other ErbB family members (10). First-generation TKIs inhibit only the EGFR signaling pathway but not other members of the ErbB family, causing tumor cells to escape and develop TKI resistance. Remarkably, TKI treatment transiently inhibited ErbB3 phosphorylation in inactive ErbB kinase family protiens (11). After temporary inhibition of TKI drugs, the ErbB3 signal is reactivated, and it is difficult to block the ErbB3/PI3K/Akt signaling pathway continuously (12). Previous studies have shown that ErbB3 plays a key role in EGFR-TKI resistance (13). As a consequence, it is worth investigating whether the reason for the limited efficacy of EGFR targeting in Kras-mutated colorectal cancer is also ErbB family activation and whether the combined targeting of multiple ErbBs can increase therapeutic efficacy.

Following this, gefitinib was first introduced into clinical use as the first generation of small-molecule compounds targeting EGFR mutations, EGFR-TKIs. Although it achieved stable results in CRC patients in phase I trials, the efficacy of gefitinib in CRC is lower than that in other types of cancer (14). However, gefitinib in combination with other EGFR-targeting agents has more impressive antitumor effects in colorectal cancer than EGFR inhibitors alone (15). Although monoclonal EGFR-TKIs, ,such as cetuximab, are more commonly used in the clinical treatment of CRC, there are still therapeutic limitations, as these drugs are ineffective in patients with RAS gene mutations (16). In fact, recent reports have shown that in patients with resectable liver metastases from colorectal cancer, the addition of cetuximab during perioperative chemotherapy significantly reduces progression-free survival (17, 18).

Nevertheless, nucleic acid drugs, such as mRNA and MicroRNAs (miRNA), target molecules that cannot be targeted by chemical drugs or antibody drugs and are expected to produce breakthrough progress on diseases treated with methods that have poor efficacy with traditional drugs (19). MiRNAs regulate the expression of target messenger RNA (mRNA) by binding to the 3'- untranslated region (3 'UTR) (20), so mutations in the CDS region do not affect miRNA downregulation of oncogene expression and promote the progression of various cancers (21). At the same time, advances in RNA molecule delivery technology have also made miRNA-based disease treatments more realistic.

In this study, we found that the protein levels of EGFR and ErbB3 were significantly increased in Kras mutant cells in the constructed colorectal cancer gefitinib resistance (GR) cell line. However, Kras wild type GR cells exhibited no significant changes in EGFR or ErbB3 protein levels. Consequently, we believe that inhibition of EGFR and ErbB3 activity is the key to improving the efficacy of targeted therapy for Kras-mutated colorectal cancer. After filtering through the database, we found that miRNA (miR-323a-3p) simultaneously targets EGFR/ErbB3, and miR-323 promoted apoptosis of colorectal cancer cells by targeting EGFR/ErbB3, reversing gefitinib resistance. This study provides a new direction for improving EGFR-targeted therapy in Kras-mutated colorectal cancer.

Methods

Cell cultures and reagents

Six human CRC cell lines were purchased from the American Type Culture Collection (ATCC, Rockville, MD, USA). HCT116/HT-29 cells were preserved in McCoy's 5A medium, HCT-8 cells were preserved in 1640 medium, LoVo cells were preserved in F-12K medium (Kaighn's Modification of Ham's F-12 Medium), and SW480/SW620 cells were preserved in Leibovitz's L-15 medium. The media were supplemented with 10% fetal bovine serum, and cells were incubated in a humidified atmosphere of 95% air and 5% CO_2 at 37°C. HCT116 GR (gefitinib-resistant), LoVo GR, SW620 GR and HT-29 GR cells were obtained by continuously culturing the cells in gefitinib (800 ng/mL) and cultured in DMEM with 10% FBS.

Transfections

Lentiviruses containing miR-323a or control were purchased from GeneChem (Shanghai, China), and the transfection of lentivirus into CRC cells was performed according to the manufacturer's protocol. After lentivirus infection, monoclonal cells were selected and cultured to check for expression of miR-323a-3p/5p by qRT-PCR. MiRNA mimics and miRNA antagomiRs were synthesized by RiboBio (Guangzhou, China) and transfected into CRC cells using Lipofectamine™ 2000 (Invitrogen, USA) according to the manufacturer's protocol.

Receptor tyrosine kinase phosphorylation profile

To investigate the activation/phosphorylation of RTKs, we used the Human RTK Phosphorylation Antibody Array Membrane (ab193662, Abcam). The human phospho-RTK antibody array is a nitrocellulose membrane with 71 different anti-RTK antibodies spotted in duplicate on it, including 4 positive and 3 negative controls and 1 blank.

To perform a proteome profiler array experiment, cell lysates were prepared from GR or NC cells using Cell Lysis Buffer supplemented with Phosphatase Inhibitor and Protease Inhibitor Cocktail and stored at −80°C until use. For each cell lysate, 200 μg of total protein (determined by the Pierce BCA Protein Assay (Fisher Scientific)) was diluted 1:5 with blocking buffer, placed onto each membrane and incubated overnight at 4°C (16 hours). The antibody array membranes were washed and subsequently incubated with biotinylated anti-phosphotyrosine antibody overnight at 4°C to detect phosphorylated tyrosine on activated receptors. After washing and incubation with HRP-streptavidin, the membranes were visualized using a chemiluminescence-based detection method.

Cell viability assay

Tumor cells ($2–3 \times 10^3$ cells/100 μL/well) in media supplemented with 10% FBS were plated in 96-well plates and cultured with the indicated compound for 72 h. After culturing, cell viability was measured using a CCK-8 kit (Dojindo Laboratories). The percentage of growth was determined relative to the untreated controls. Experiments were repeated at least three times with triplicate samples.

Patients and bioinformatics analysis

Paired colorectal tumor tissues and their corresponding adjacent nontumor colorectal tissues (5 cm away from the lesions) were collected from patients who underwent curative surgery for CRC at Renji Hospital,

Shanghai, China. A CRC diagnosis was confirmed by histological examination, and the relevant clinical and pathological information was retrieved from the hospital database. The expression of miRNAs in CRC and normal controls was determined using the TCGA database, and a heat map and volcano map were acquired using R.

RNA extraction and quantitative real-time RT-PCR (qRT-PCR)

Total RNA was extracted from cell lines and frozen tumor samples using TRIzol reagent (Invitrogen, Carlsbad, CA). cDNA was reverse-transcribed from 1 μg of RNA using a SYBR® Prime ScriptTM RT-PCR kit (Takara Biochemicals, Tokyo, Japan), and quantitative PCR was performed using SYBR Select Master Mix (Roche, Switzerland) and gene-specific primers on an ABI PRISM® 7500HT Real-Time PCR System. The thermal cycling conditions were as follows: an initial step at 95°C for 15 s followed by 40 cycles of 95°C for 5 s and 60°C for 30 s. Each experiment was performed in a 20-μl reaction volume containing 10 μl of SYBR® Prime Ex TaqTM II (2×), 1 μl of forward primer and reverse primer (10 μM each), 2 μl of cDNA, and 7 μl of H2O. β-Actin was used as an internal control. The quantification of the mRNA was calculated using the comparative Ct (the threshold cycle) method according to the following formula: Ratio = $2^{-\Delta\Delta CT} = 2^{-[\Delta Ct(sample)-\Delta Ct(calibrator)]}$, where ΔCt is equal to the Ct of the target gene minus the Ct of the endogenous control gene (β-actin). The primers were as follows: EGFR (F: 5'-CCAAGGCACGAGTAACAAGC-3’; R: 5'- TCCCAAGGACCACCTCACAG-3’); ErbB3 (F: 5’-GGTGATGGGGAACCTTGAGAT-3’; R: 5’-CTGTCACTTCTCGAATCCACTG-3’)

EGFR T790M mutation detection

We purchased all probe qPCR mix (or UNG) reagents from Takara (Tokyo, Japan) and custom ordered primers and probes from GENEWIZ (Guangzhou, China). We performed probe qPCR analysis on an ABI PRISM®7500HT Real-Time PCR System as previously described under the following PCR conditions: EGFR T790M: forward primer, 5'-GCCTGCTGGGCATCTG-3', reverse primer, 5'-TCTTTGTGTTCCCGGACATAGTC-3'. The probe sequences were 5'-VIC-ATGAGCTGCGTGATGAG-MGB-NFQ-3' and 5'-FAM-ATGAGCTGCATGATGAG-MGB-NFQ-3'. Cycling conditions: 95°C × 10 min (1 cycle), 40 cycles of 94°C × 30 s and 58°C × 1 min, followed by a 10°C hold.

Antibodies and western blotting

Protein aliquots of 25 μg each were resolved by SDS polyacrylamide gel electrophoresis (Bio-Rad, Hercules, CA) with the appropriate antibodies. Electrophoresed protein samples were transferred to polyvinylidene difluoride membranes (Bio-Rad). After being washed three times, the membranes were incubated in blotting-grade blocker (Bio-Rad) for 1 h at room temperature and overnight at 4°C with primary antibodies to t-EGFR, p-EGFR, t-ErbB3, p-ErbB3, t-PI3K, p-PI3K, p-Akt, t-Akt, t-Erk1/2, p-Erk1/2, t-GSK3β,p-GSK3β,MMP9,PCNA,p21, Caspase-3, Cleaved-Caspae-3, Caspase-7, Cleaved-Caspase-7, Caspase-9, Cleaved-Caspase-9, and β-actin (1:1,000 dilution; Cell Signaling Technology, Danvers, MA, USA). After being washed three times, the membranes were incubated for 1 h at room temperature with HRP-conjugated species-specific secondary antibody. Immunoreactive bands were visualized using

SuperSignal West Dura Extended Duration Substrate Enhanced Chemiluminescent Substrate (Pierce Biotechnology). Each experiment was independently performed at least three times.

Cell proliferation

The RTCA xCELLigence system (ACEA Biosciences Inc., The Netherlands) was used to measure cell proliferation in real time. CRC cells were placed at a density of 4000–8000/well, and E-plates were then transferred to the RTCA instrument for automated real-time monitoring under standard incubator conditions. Cell proliferation was monitored every 30 minutes. After 72 h, the measurement was stopped, and the results were analyzed using RTCA software. To check the influence of exosomes from miR-323a-3p-overexpressing HCT116 cells on cell proliferation, CRC cells were first plated at a density of 4000–8000/well. After 24 h, exosomes from control or miR-323a-3p-overexpressing HCT116 cells were added, the measurement was stopped, and the results were analyzed after an additional 24 h.

Colony formation assay

Transfected CRC cells were seeded into 6-well plates at a density of 200 to 800 cells per well and incubated for 2 weeks. The cells were fixed and stained in a dye solution containing 0.1% crystal violet and 100% methanol. The number of colonies was subsequently counted and analyzed.

Flow cytometry

Apoptosis was determined by fluorescence-activated cell sorting (FACS) flow cytometry. The transfected cells collected after trypsinization were washed twice with PBS and resuspended in 1X binding buffer. Cells were then stained using 10 μL FITC-labeled buffer for 20 minutes and 10 μL PE-labeled buffer for 5 minutes according to the manufacturer's instructions. The apoptosis rate was analyzed by FACS flow cytometry (BD Biosciences, Heidelberg, Germany).

Luciferase reporter assay

HCT116 cells grown in 24-well plates were cotransfected with luciferase reporter (200 ng per well), miR-323a-3p-mimic (200 ng per well), and 10 ng *Renilla* using Lipofectamine™ 2000. Forty-eight hours later, a Dual-Luciferase Reporter Assay kit (Promega, USA) was used to measure the luciferase and Renilla activities according to the manufacturer's instructions. The relative luciferase activity was determined using BioTek Syngery 2 (BioTek, USA), and the transfection efficiency was normalized to Renilla activity.

CDX models

Suspensions of 3×10^6 cells were injected subcutaneously into the flanks of four-week-old nude mice. Once the mean tumor volume reached ~ 50–100 mm^3, the mice were orally administered gefitinib and injected with agomir three times per week. Tumors were measured three times per week using calipers, and tumor volumes were calculated as $width^2 \times length/2$. Mice were euthanized after 28 days, tumors were collected and weighed, and total RNA and protein were prepared from tumor tissues for qRT-PCR and western blot analysis.

Results

EGFR/ErbB3 is significantly activated in gefitinib-resistant Kras mutant CRC cell lines, and ErbB3 is upregulated in Kras mutant CRC tissues

Initially, we constructed four groups of CRC-GR cell lines, Kras mutant cells (HCT116, LoVo, and SW620) and Kras wild type cells (HT-29), and the dose of gefitinib resistance reached 50 μm. After preliminary screening of the four groups of cells by phosphorylated RTK antibody array, 16 proteins were observed to exhibit altered phosphorylation levels in gefitinib-resistant cell lines. Statistical analysis revealed that EGFR and ErbB3 levels were changed in all three groups of Kras mutant cells (Fig. 1A and Fig. S1F). ErbB mRNA levels were analyzed in drug-resistant cell lines (Fig. 1B), and the data showed that the mRNA levels of both EGFR and ErbB3 were significantly increased in all four groups, while ErbB2/ErbB4 were not significantly changed. Furthermore, EGFR/ErbB3 protein levels were detected in four drug-resistant cell lines, and the data showed that total protein expression levels of EGFR and ErbB3 in GR Kras mutant cell lines were significantly increased, indicating that both EGFR and ErbB3 were significantly activated. However, the total and phosphorylated protein levels of EGFR/ErbB3 in HT-29 cell lines were not significantly changed (Fig. 1C). We also checked for the possible EGFR T790M mutation during TKI resistance, and no change in mutation level was detected in either the subcutaneous tumor model or in drug-resistant cells (Fig. S1B).

To investigate the significance of EGFR and ErbB3 in Kras-mutant CRC, we analyzed the expression of EGFR and ErbB3 in the TCGA database and the relationship with prognosis. The data showed that ErbB3 was the third most altered of 122 upregulated genes in Kras mutant tissues compared to other types CRC mutations (Fig. 1E). Further analysis showed that in CRC patients with high ErbB3 expression, high expression of EGFR was associated with a poorer prognosis than low expression of EGFR (Fig. 1D). Independent analysis of EGFR and ErbB3 revealed no correlation between EGFR expression and prognosis.

Overall, these data indicate that ErbB3 is highly expressed in tissues of patients with Kras mutations and in Kras mutant GR cell lines.

MiR-323a-3p directly targets EGFR/ErbB3 and inhibits CRC cell proliferation in vitro and tumor growth in vivo

To solve the limitations of Kras mutation in current clinical use of TKIs in CRC, we attempted to find microRNAs that can target both EGFR and ErbB3 and inhibit the expression of these two genes to improve the efficacy of targeted therapy. Combining four miRNA target molecular databases (TargetScan, HMDD, miRgator, and miRDB) for comprehensive analysis, miR-323a-3p was selected as our candidate microRNA (Fig. 2A). Next, a luciferase reporter assay was used to verify that miR-323a-3p directly binds to the 3’UTR of EGFR and ErbB3, and the inhibitory effect of miR-323a-3p on target genes was further verified in HCT116 cell lines (Fig. 2B and Fig. 2C). For Kras wild type CRC cells (HCT-8), the inhibitory effect of miR-323a-3p on target genes was also significant (Fig. S1D).

To determine the biological significance of miR-323a-3p in CRC, we analyzed miR-323a-3p expression and its relationship with prognosis in the TCGA database. The data showed that miR-323a-3p was expressed at low levels in CRC tissues (Fig. 2D), and this low expression was associated with poor prognosis in colorectal cancer (Fig. 1E). Then, we validated the miR-323a-3p expression levels by Quantitative real-time polymerase chain reaction (qRT-PCR) assay, and miR-323a-3p was significantly downregulated in CRC tissues compared to their adjacent tissues in our cohort (n=36, Fig. 2F).

Furthermore, we explored miR-323a-3p function in CRC cells. The results showed that the overexpression of miR-323a-3p in CRC cells significantly inhibited cell proliferation (Fig. 2H). Similarly, Kras wild type cells (HCT-8) also showed some inhibition (Fig. S2B). We also conducted a clone formation assay and observed that CRC cells transfected with miR-323a-3p formed significantly fewer clones than control cells (Fig. 2G). Moreover, miR-323a-3p also inhibited the migration and invasion of CRC cells (Fig. S2D and E). Significant differences in cell proliferation levels were observed after transfection of anti-miR-323a-3p into HCT116 and HCT-8 cells. After anti-miR-323a-3p transfection with HCT-8, the colony number and proliferation level increased, while HCT116 transfection caused no significant change (Fig. S2F).

Subsequently, we examined the effect of miR-323a-3p on the biological characteristics of CRC cells in vivo. We subcutaneously injected miR-323a-3p-overexpressing cell lines or control HCT116 cells into nude mice. As shown in Fig. 2I and Fig. S2G, 6 weeks after the injection of HCT116 cells overexpressing miR-323a-3p, compared to the control group, the tumor volume inhibition rate was 75%, and the tumor weight inhibition rate was 71%. In addition, the expression level of miR-323a-3p was detected in the tumor tissue of mice injected with HCT116 cells and was increased in the tumor tissue of mice injected with HCT116 cells transfected with miR-323a-3p (TUZHU).

In conclusion, these data indicate that low expression of miR-323a-3p is associated with poor prognosis in colorectal cancer. Overexpression of miR-323a-3p inhibits cell growth by targeting EGFR and ErbB3 directly in vivo and in vitro. Therefore, miR-323a-3p represents a tumor suppressor microRNA that inhibits EGFR/ErbB3 and improves the efficacy of targeted therapy for colorectal cancer.

MiR-323a-3p inhibits tumor growth by promoting apoptosis in CRC in vitro and in vivo

To further understand the function of miR-323a-3p, we performed hallmark gene enrichment analysis using RNA-seq data from miR-323a-3p-overexpressing cell lines. The data revealed that apoptosis was the second pathway in these enrichment pathways (Fig. 3a). Then, we detected changes in apoptosis-related proteins (caspase3/7/9) after administration of the miR-323a-3p agomir. The results showed that the levels of apoptotic markers were activated in HCT116 cells and subcutaneous tumors in response to overexpression miR-323a-3p (Fig. 3B and C). Similar results were obtained in HCT-8 cells (Fig. S3C).

To investigate the apoptotic function of miR-323a-3p in CRC, we selected 6 CRC cell lines (HCT116, LoVo, SW480, SW620, HCT-8 and HT-29) for flow cytometry analysis, and the results showed that the miR-323a-3p agomir had apoptotic effects on all 6 types of cells (Fig. 3D and E). Similar results were obtained for the changes in proliferation of the 6 types of cells by the detection of RTCA cell growth (Fig. 3F and Fig.

S3a). Furthermore, we detected changes in target gene protein levels between cell lines after administration of agomir (Fig. 3G).

The above results indicated that miR-323a-3p inhibits cell proliferation by directly targeting EGFR and ErbB3 to induce apoptosis.

MiR-323a-3p inhibits EGFR/ErbB3 activation in GR CRC cells

ErbB3 is highly expressed in Kras mutant CRC tissues, enabling them to escape EGFR-TKI inhibition. EGFR/ErbB3 was activated in Kras mutant GR CRC cells and escaped gefitinib inhibition. MiR-323a-3p inhibited tumor growth in acquired GR Kras mutant cell lines and ErbB3 high expression Kras mutant CRC tissues by inhibiting the expression of EGFR and ErbB3.

First, the EGFR/ErbB3 inhibition rate of gefitinib was detected in the GR cell lines. Although p-EGFR in drug-resistant cell lines was reduced in response to treatment with 200 nM gefitinib for 48 h, protein levels of p-ErbB3 did not significantly change (Fig. 4B). However, the phosphorylated protein levels of EGFR/ErbB3 were significantly reduced after adding agomir for 72 h, and based on this, we found that the inhibitory effect of gefitinib and agomir was more significant (Fig. 4C). In addition, similar results were obtained in the Kras wild type cell line (HT-29) (Fig. S3D).

These results indicated that the upregulated phosphorylated EGFR/ErbB3 level of Kras mutant CRC cells after drug resistance could no longer be controlled at the effective level by TKIs, and the downstream PI3K/Akt pathway continued to be activated. However, the inhibitory effect of agomir on EGFR/ErbB3 in GR CRC cells was not affected, and the inhibitory effect was enhanced after simultaneous administration of agomir and gefitinib.

The molecular regulatory network of miR-323a-3p

MiR-323a-3p targets EGFR/ErbB3, promotes apoptosis, inhibits tumor growth in vivo and in vitro, and reverses GR due to its dual-targeting properties. However, its molecular mechanism has not yet been elucidated, so we continued to analyze the RNA-sequencing data of miR-323a-3p-overexpressing HCT116 cells and conducted a pathway analysis by combining the findings with the KEGG database (Fig. 5A). The results demonstrated that the differentially expressed genes were enriched in multiple EGFR/ErbB3-related pathways. Then, we detected the mRNA expression profile by RNA-seq, and the data showed that 88 genes were downregulated in miR-323a-3p HCT-116 cells compared to the control group (Fig. 5B). Then, we detected the expression of these genes in overexpressed HCT116 and HCT-8 cells by qRT-PCR (Fig. 5B), and the results showed that EGFR and ErbB3 were significantly downregulated. Then, we verified the protein level changes of the significantly different genes (PI3K, c-FOS, Akt, GSK-3β, ERK1/2, MMP9, PCNA and p21) through western blot and constructed a protein interaction network of the different genes in the above sequencing results using WEB-String (Fig. 5C and D). These results reveal the changes in the primary downstream phosphorylation levels of miR-323a-3p targeting EGFR/ErbB3 and

the resulting molecular regulatory network. In addition, the rescue experiment we conducted with an EGFR agonist (NSC228155) is shown in Figure S4.

MiR-323a-3p and gefitinib synergistically inhibit CRC cell proliferation

Interestingly in the process of solving the drug resistance problem, we found that miR-323a-3p not only relieved CRC GR but also showed a stronger inhibitory effect on p-EGFR/p-ErbB3 protein levels in combination with gefitinib and miR-323a-3p than in the single administration group (Fig. 4C and Fig. 5A). Consequently, when exploring the apoptotic function of miR-323a-3p, we also attempted to combine gefitinib and miR-323a-3p and found that they had a strong effect on promoting apoptosis in CRC cells. Based on Bliss data analysis, the optimal concentration of the combination was finally determined (Fig. 5D). Reviewing the clinical trial data of gefitinib in the early stage of CRC, we found that, unlike the obvious effect of cetuximab on tumor size, previous studies found that the ErbB3/PI3K/Akt pathway also plays a negative regulatory role in trastuzumab-mediated p27Kip1-mediated G1 cell cycle arrest in breast cancer [14]. The lack of ErbB3 expression in poorly differentiated colorectal cancer cells enhances gefitinib sensitivity [15]. The antitumor mechanism of gefitinib is the promotion of cell cycle arrest and the reduction of the expression of tumor metastasis-related proteins [6] rather than the direct effect of miR-323a-3p on CRC cell apoptosis. This may also explain why gefitinib has long been a poor treatment for CRC. In this study, the synergistic effect of gefitinib and miR-323 in the combined treatment group was pro-apoptotic (Fig. 5B and C) based on the cell cycle arrest effect of gefitinib [7] and miR-323 promoting apoptosis through 3'- UTR binding to the EGFR/ErbB3 target gene. In addition, two inhibitors targeting individual ErbB family members have been shown to have significantly higher antitumor activity than single drug therapy alone [2].

MiR-323a-3p and gefitinib synergistically inhibit tumor growth, and miR-323a-3p blocks the formation acquired gefitinib resistance in a xenograft model

At present, clinical TKI treatment is ineffective for Kras mutant CRC, while agomir has a significant proapoptotic effect at the cellular level showing a synergy in combination with gefitinib on the proapoptotic effect. Therefore, we next evaluated the effect of miR-323a-3p combined with gefitinib on the growth of subcutaneous tumor HCT116 cells. Subcutaneous tumors grew rapidly from HCT116 cells, and gefitinib monotherapy did not inhibit their growth. Treatment with agomir after peritumor injection resulted in tumor shrinkage. These tumors rapidly regrew after discontinuation of agomir (Fig. 7A, B). After combined administration of miR-323a-3p and gefitinib, the subcutaneous tumors composed of HCT116 cells maintained a period of growth arrest, and the survival time was much longer than that of the monotherapy group.

Additionally, the HCT116 subcutaneous tumor model showed similar results in tumor weight and volume four weeks after administration (Fig. 7D, E), but the tumor weight and volume were slightly decreased after administration of miR-323a-3p or gefitinib, with tumor growth inhibition rates of 27% and 33%, respectively. After combination administration, tumor weight and volume were smaller than those of the single administration group, and tumor growth remained stagnant. The EGFR/ErbB3 protein expression

results were also consistent with the cell experiments, indicating the synergistic effect of the combination drug treatment. More meaningfully, we extracted four groups of subcutaneous tumors for the generation of cell culture and the treatment of IC50 detection. The results showed that the single IC50 agomir group exhibited 47% inhibition compared to the control group. Furthermore, treatment for four weeks after lavage treatment, the primary cell IC50 increased by 52% compared to the control group, and the combination group of IC50 values were much lower than the single drug groups, up by 59% compared to the control group.

The above results indicate that the reversal of GR by agomir was not limited to the occurrence of drug resistance but also suggested that miR-323a-3p may prevent the formation of drug resistance by maintaining low levels of EGFR/ErbB3.

Discussion

In this study, EGFR/ErbB3 was significantly activated in drug-resistant Kras mutant colorectal cancer cell lines, and ErbB3 was highly expressed in Kras mutant CRC tissues. MiR-323a-3p simultaneously targeted EGFR/ErbB3, inhibited the growth of colorectal cancer cell lines by promoting apoptosis, prevented the formation of drug resistance in colorectal cancer cell lines and reversed EGFR-targeting drug resistance, suggesting that miR-323a-3p may improve the EGFR-targeting therapeutic effect in colorectal cancer, especially Kras mutant colorectal cancer.

Acquired TKI resistance is primarily divided into three types: EGFR second site T790M mutation, bypass activation and phenotypic transformation (22, 23), and ErbBs are involved in these processes (24–26). In the non-small cell lung cancer model system, EGFR has L858R and T790M mutations and is resistant to cetuximab (27, 28), with upregulated NRG and HER3-driven resistance. In CRC PDX models, the EGFR family was also found to undergo adaptive reprogramming through other mechanisms following EGFR inhibition: upregulation of BTC or MYC-related HER3 expression independent of YAP (29, 30). In addition, the amplification of the MET oncogene in NSCLC during EGFR-TKI treatment induces HER3 activation through coupling, maintaining activation of the PI3K/Akt cell survival signaling pathway(31, 32). However, in this study, we found that the phosphorylated protein level of EGFR/ErbB3 in Kras mutant GR CRC cells was significantly increased, suggesting that ErbB3 may be an important target for the treatment of Kras mutant colorectal cancer.

Mutations in Kras, BRAF, BIM polymorphism deficiency and EML4-ALK fusion gene mutations are the primary resistance mechanisms against EGFR inhibitors (33). In a PDX model of mouse lung adenocarcinoma, Emilio's team found that EGFR signaling is involved in K-Ras-driven lung tumorigenesis in both humans and mice. In their TKI-resistant model, EGFR and ErbB3 were significantly activated, and the loss of EGFR quenched mutated Kras activity and temporarily reduced tumor growth. In this study, we found that EGFR/ErbB3 was significantly activated in TKI-resistant models of colorectal cancer, and this activation had shared specific aspects of colorectal cancers; that is, it was primarily concentrated in Kras-

mutated colorectal cancer, which may be one of the reasons for the poor therapeutic effect of TKIs in colorectal cancer.

Current TKI therapies use small-molecule inhibitors that target only proteins and inhibit the phosphorylation of ErbB3, a kinase-inactive family member, only briefly and have difficulty blocking the HER3/PI3K/Akt signaling pathway on a sustained basis (34). However, miRNAs are small molecules that lack immunogenicity and exhibit multiple regulatory functions at the level of mRNA and protein translation (35). MiR-323a-3p directly degraded EGFR/ErbB3 mRNA, and T-EGFR/T-ErbB3 protein was stably inhibited at a low level. Furthermore, the bypass signaling pathway was difficult to activate, even after the occurrence of drug resistance.

ErbB3 plays a key regulatory role in downstream signal transduction of the PI3K/Akt pathway. Recent studies have shown that ErbB3 overexpression and consequent activation of PI3K/Akt signaling lead to HER2-overexpressing breast cancers becoming resistant to tyrosine kinase inhibitors (31, 36), such as gefitinib, and tumor cells have finally found a way to bypass the blockade of targeted therapy. In the present study, our gefitinib-resistant CRC cell model showed similar results: gefitinib showed minimal effects in controlling PI3K/Akt phosphorylation. However, miR-323a-3p inhibits EGFR and ErbB3 mRNA levels, and ErbB3 can no longer regulate downstream signals through multiple docking sites with PI3K's p85 regulatory subunit and dimerization with other HER2 members.

Overall, we found that Kras mutant CRC TKI resistance occurs due to the activation of EGFR and ErbB3. MiR-323 targeting these two important targets raises the possibility of an EGFR-TKI-based strategy for the treatment of Kras-mutated colorectal cancer, which is prone to drug resistance. MiR-323 is of long-term significance both after the occurrence of TKI resistance and during the progression of TKI resistance. In addition to its own proapoptotic and anticancer effects, miR-323 combined with gefitinib exhibited impressive synergistic proapoptotic effects.

Conclusion

Collectively, it was drawn from this research that ErbB3 and EGFR were activated in gefitinib-resistant Kras mutant CRC cells, thus to promote the progress of Tki-resistance. MiR-323a-3p targeting EGFR/ErbB3 inhibited Kras mutant CRC tumor growth and gefitinib resistance acquisition.

Abbreviations

Colorectalcancer CRC

overall survival OS

tyrosine kinase inhibitors TKI

MicroRNAs miRNA

drug resistance GR

Quantitative real-time polymerase chain reaction qRT-PCR

Declarations

Availability of data and materials

Related data and materials have been shown in the present manuscript and supplementary files.

Funding

The study was supported by the Natural Science Foundation of China(81572454).

Author notes

Yuanzhou Zhang and Shunshun Liang are co-first authors

Contributions

XL, YZ: manuscript editing, review and data analysis. BX, JH and YZ: data collection and experiments. SL, LW: figures preparation. All authors read and approved the final manuscript.

Ethics approval and consent to participate

This study was approved and supervised by the animal ethics committee of Shanghai Cancer Institute. The treatment of animals in all experiments conforms to the ethical standards of experimental animals.

Consent for publication

Not applicable.

Competing interests

The authors declare that they have no competing interests.

Acknowledgements

We are very grateful to all individuals and groups involved in this study.

References

1. Jemal A, Bray F, Center MM, Ferlay J, Ward E, Forman D. Global cancer statistics. CA: a cancer journal for clinicians. 2011;61(2):69-90.
2. Arnold M, Sierra MS, Laversanne M, Soerjomataram I, Jemal A, Bray F. Global patterns and trends in colorectal cancer incidence and mortality. Gut. 2017;66(4):683-91.

3. Zhao S, Mi Y, Guan B, Zheng B, Wei P, Gu Y, et al. Tumor-derived exosomal miR-934 induces macrophage M2 polarization to promote liver metastasis of colorectal cancer. Journal of hematology & oncology. 2020;13(1):156.
4. Tang X, Sun G, He Q, Wang C, Shi J, Gao L, et al. Circular noncoding RNA circMBOAT2 is a novel tumor marker and regulates proliferation/migration by sponging miR-519d-3p in colorectal cancer. Cell death & disease. 2020;11(8):625.
5. Du F, Cao T, Xie H, Li T, Sun L, Liu H, et al. KRAS Mutation-Responsive miR-139-5p inhibits Colorectal Cancer Progression and is repressed by Wnt Signaling. Theranostics. 2020;10(16):7335-50.
6. Byrne M, Saif MW. Selecting treatment options in refractory metastatic colorectal cancer. OncoTargets and therapy. 2019;12:2271-8.
7. Yaeger R, Chatila WK, Lipsyc MD, Hechtman JF, Cercek A, Sanchez-Vega F, et al. Clinical Sequencing Defines the Genomic Landscape of Metastatic Colorectal Cancer. Cancer cell. 2018;33(1):125-36.e3.
8. Bronte G, Cicero G, Cusenza S, Galvano A, Musso E, Rizzo S, et al. Monoclonal antibodies in gastrointestinal cancers. Expert opinion on biological therapy. 2013;13(6):889-900.
9. Xie J, Xia L, Xiang W, He W, Yin H, Wang F, et al. Metformin selectively inhibits metastatic colorectal cancer with the KRAS mutation by intracellular accumulation through silencing MATE1. Proceedings of the National Academy of Sciences of the United States of America. 2020;117(23):13012-22.
10. Moll HP, Pranz K, Musteanu M, Grabner B, Hruschka N, Mohrherr J, et al. Afatinib restrains K-RAS-driven lung tumorigenesis. Science translational medicine. 2018;10(446).
11. Sergina NV, Rausch M, Wang D, Blair J, Hann B, Shokat KM, et al. Escape from HER-family tyrosine kinase inhibitor therapy by the kinase-inactive HER3. Nature. 2007;445(7126):437-41.
12. Engelman JA, Mukohara T, Zejnullahu K, Lifshits E, Borras AM, Gale CM, et al. Allelic dilution obscures detection of a biologically significant resistance mutation in EGFR-amplified lung cancer. The Journal of clinical investigation. 2006;116(10):2695-706.
13. Yonesaka K, Takegawa N, Watanabe S, Haratani K, Kawakami H, Sakai K, et al. An HER3-targeting antibody-drug conjugate incorporating a DNA topoisomerase I inhibitor U3-1402 conquers EGFR tyrosine kinase inhibitor-resistant NSCLC. Oncogene. 2019;38(9):1398-409.
14. Blanke CD. Gefitinib in colorectal cancer: if wishes were horses. Journal of clinical oncology : official journal of the American Society of Clinical Oncology. 2005;23(24):5446-9.
15. Yuan HH, Han Y, Bian WX, Liu L, Bai YX. The effect of monoclonal antibody cetuximab (C225) in combination with tyrosine kinase inhibitor gefitinib (ZD1839) on colon cancer cell lines. Pathology. 2012;44(6):547-51.
16. Parseghian CM, Loree JM, Morris VK, Liu X, Clifton KK, Napolitano S, et al. Anti-EGFR-resistant clones decay exponentially after progression: implications for anti-EGFR re-challenge. Annals of oncology : official journal of the European Society for Medical Oncology. 2019;30(2):243-9.
17. Bridgewater JA, Pugh SA, Maishman T, Eminton Z, Mellor J, Whitehead A, et al. Systemic chemotherapy with or without cetuximab in patients with resectable colorectal liver metastasis (New

EPOC): long-term results of a multicentre, randomised, controlled, phase 3 trial. The Lancet Oncology. 2020;21(3):398-411.

18. Gholami S, Grothey A. EGFR antibodies in resectable metastatic colorectal liver metastasis: more harm than benefit? The Lancet Oncology. 2020;21(3):324-6.
19. Scott LJ. Givosiran: First Approval. Drugs. 2020;80(3):335-9.
20. Toyoshima S, Sakamoto-Sasaki T, Kurosawa Y, Hayama K, Matsuda A, Watanabe Y, et al. miR103a-3p in extracellular vesicles from FcepsilonRI-aggregated human mast cells enhances IL-5 production by group 2 innate lymphoid cells. The Journal of allergy and clinical immunology. 2021;147(5):1878-91.
21. Ghafouri-Fard S, Shoorei H, Mohaqiq M, Majidpoor J, Moosavi MA, Taheri M. Exploring the role of non-coding RNAs in autophagy. Autophagy. 2021:1-22.
22. Russo M, Crisafulli G, Sogari A, Reilly NM, Arena S, Lamba S, et al. Adaptive mutability of colorectal cancers in response to targeted therapies. Science. 2019;366(6472):1473-80.
23. Hata AN, Niederst MJ, Archibald HL, Gomez-Caraballo M, Siddiqui FM, Mulvey HE, et al. Tumor cells can follow distinct evolutionary paths to become resistant to epidermal growth factor receptor inhibition. Nature medicine. 2016;22(3):262-9.
24. Arteaga CL, Engelman JA. ERBB receptors: from oncogene discovery to basic science to mechanism-based cancer therapeutics. Cancer cell. 2014;25(3):282-303.
25. Tebbutt N, Pedersen MW, Johns TG. Targeting the ERBB family in cancer: couples therapy. Nature reviews Cancer. 2013;13(9):663-73.
26. Lupo B, Sassi F, Pinnelli M, Galimi F, Zanella ER, Vurchio V, et al. Colorectal cancer residual disease at maximal response to EGFR blockade displays a druggable Paneth cell-like phenotype. Science translational medicine. 2020;12(555).
27. Wang Y, Yang N, Zhang Y, Li L, Han R, Zhu M, et al. Effective Treatment of Lung Adenocarcinoma Harboring EGFR-Activating Mutation, T790M, and cis-C797S Triple Mutations by Brigatinib and Cetuximab Combination Therapy. Journal of thoracic oncology : official publication of the International Association for the Study of Lung Cancer. 2020;15(8):1369-75.
28. Della Corte CM, Ciaramella V, Cardone C, La Monica S, Alfieri R, Petronini PG, et al. Antitumor Efficacy of Dual Blockade of EGFR Signaling by Osimertinib in Combination With Selumetinib or Cetuximab in Activated EGFR Human NCLC Tumor Models. Journal of thoracic oncology : official publication of the International Association for the Study of Lung Cancer. 2018;13(6):810-20.
29. Kim ST, Klempner SJ, Park SH, Park JO, Park YS, Lim HY, et al. Correlating programmed death ligand 1 (PD-L1) expression, mismatch repair deficiency, and outcomes across tumor types: implications for immunotherapy. Oncotarget. 2017;8(44):77415-23.
30. Kurppa KJ, Liu Y, To C, Zhang T, Fan M, Vajdi A, et al. Treatment-Induced Tumor Dormancy through YAP-Mediated Transcriptional Reprogramming of the Apoptotic Pathway. Cancer cell. 2020;37(1):104-22 e12.

31. Yakes FM, Chinratanalab W, Ritter CA, King W, Seelig S, Arteaga CL. Herceptin-induced inhibition of phosphatidylinositol-3 kinase and Akt Is required for antibody-mediated effects on p27, cyclin D1, and antitumor action. Cancer research. 2002;62(14):4132-41.
32. Ramalingam SS, Vansteenkiste J, Planchard D, Cho BC, Gray JE, Ohe Y, et al. Overall Survival with Osimertinib in Untreated, EGFR-Mutated Advanced NSCLC. The New England journal of medicine. 2020;382(1):41-50.
33. Zheng GW, Tang MM, Shu CY, Xin WX, Zhang YH, Chi BB, et al. A small natural molecule CADPE kills residual colorectal cancer cells by inhibiting key transcription factors and translation initiation factors. Cell death & disease. 2020;11(11):982.
34. Nakata S, Tanaka H, Ito Y, Hara M, Fujita M, Kondo E, et al. Deficient HER3 expression in poorly-differentiated colorectal cancer cells enhances gefitinib sensitivity. International journal of oncology. 2014;45(4):1583-93.
35. Lv Y, Huang Y, Xu M, Heng BC, Yang C, Cao C, et al. The miR-193a-3p-MAP3k3 Signaling Axis Regulates Substrate Topography-Induced Osteogenesis of Bone Marrow Stem Cells. Advanced science. 2020;7(1):1901412.
36. Claus J, Patel G, Ng T, Parker PJ. A role for the pseudokinase HER3 in the acquired resistance against EGFR- and HER2-directed targeted therapy. Biochemical Society transactions. 2014;42(4):831-6.

Figures

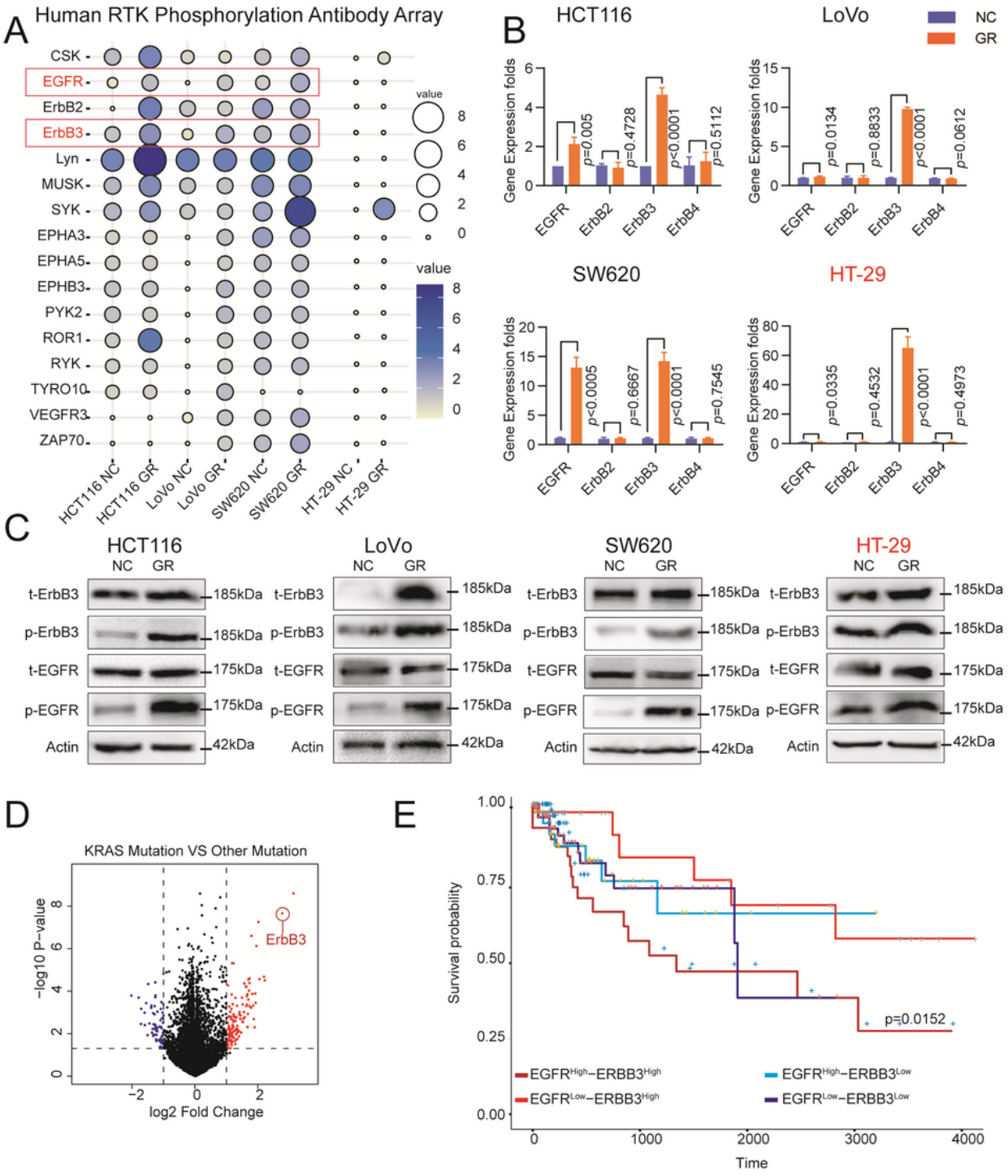

Figure 1

EGFR/ErbB3 is significantly activated in gefitinib-resistant KRAS mutant CRC cell lines, and ErbB3 is upregulated in KRAS mutant CRC tissues. A. Phosphorylation levels of EGFR and ErbB3 were both upregulated in KRAS mutant cell lines (HCT-116, LoVo and SW620) and were not changed in the KRAS non-mutant HT-29 cell line. B. EGFR/ErbB3 mRNA expression levels were significantly increased in gefitinib-resistant cell lines, while ErbB2/ErbB4 did not change significantly. Bars indicate s.d. of triplicate

cultures. Data are presented as the mean ± s.d. C. Total protein expression levels of EGFR and ErbB3 in GR KRAS mutant cell lines were significantly increased, and EGFR and ErbB3 were significantly activated. However, total and phosphorylated protein levels of EGFR/ErbB3 in HT-29 cell lines showed no significant changes. D. Simultaneous high expression of EGFR and ErbB3 is associated with poor prognosis in CRC patients (TCGA datasets). E. ErbB3 is highly expressed in KRAS mutant colorectal cancer tissues.

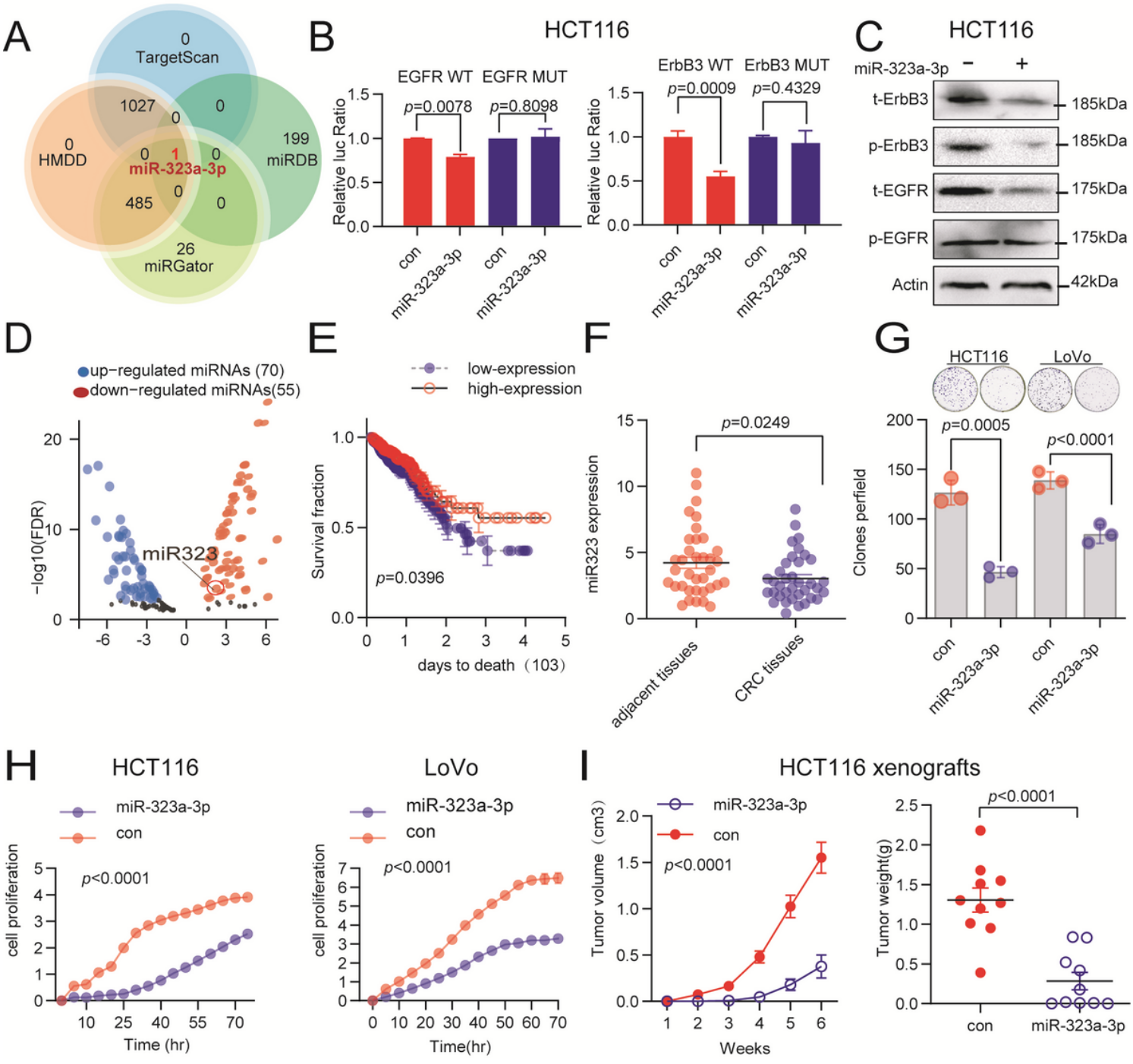

Figure 2

MiR-323a-3p directly targets EGFR/ErbB3 and inhibits CRC cell proliferation in vitro and tumor growth in vivo. A. Four microRNA targeting molecule prediction databases were analyzed for EGFR/ErbB3-targeting microRNAs, and miR-323-3p was found to simultaneously target EGFR/ErbB3 in all four databases. B.

Fluorescence reporter assays revealed that miR-323-3p binds to the wild type EGFR/ErbB3 3'-UTR but could not bind to mutant EGFR/ErbB3 3'-UTR. C. MiR-323a-3p inhibits total and phosphorylated EGFR/ErbB3 levels in HCT-116 cells. D. MiR-323a-3p is low expression in CRC tissues. E. Low miR-323a-3p expression in CRC tissues is associated with poor prognosis. F. Low miR-323a-3p expression was validated in CRC tissues by qRT-PCR assay in CRC tissues (compared to adjacent tissues, n=36). G. Overexpression of miR-323a-3p in CRC cells reduced clone formation. A colony formation assay was performed after transfection of HCT116 and LoVo cells with control and miR-323a-3p lentiviruses (n=3 per group). H. Overexpression of miR-323a-3p inhibits CRC cell proliferation. Cell proliferation capacity of HCT116 and LoVo cells after transfection with control or miR-323a-3p lentiviruses (n=3 per group). I. Growth was inhibited in subcutaneous tumors inoculated with HCT116 cells overexpressing miR-323a-3p.

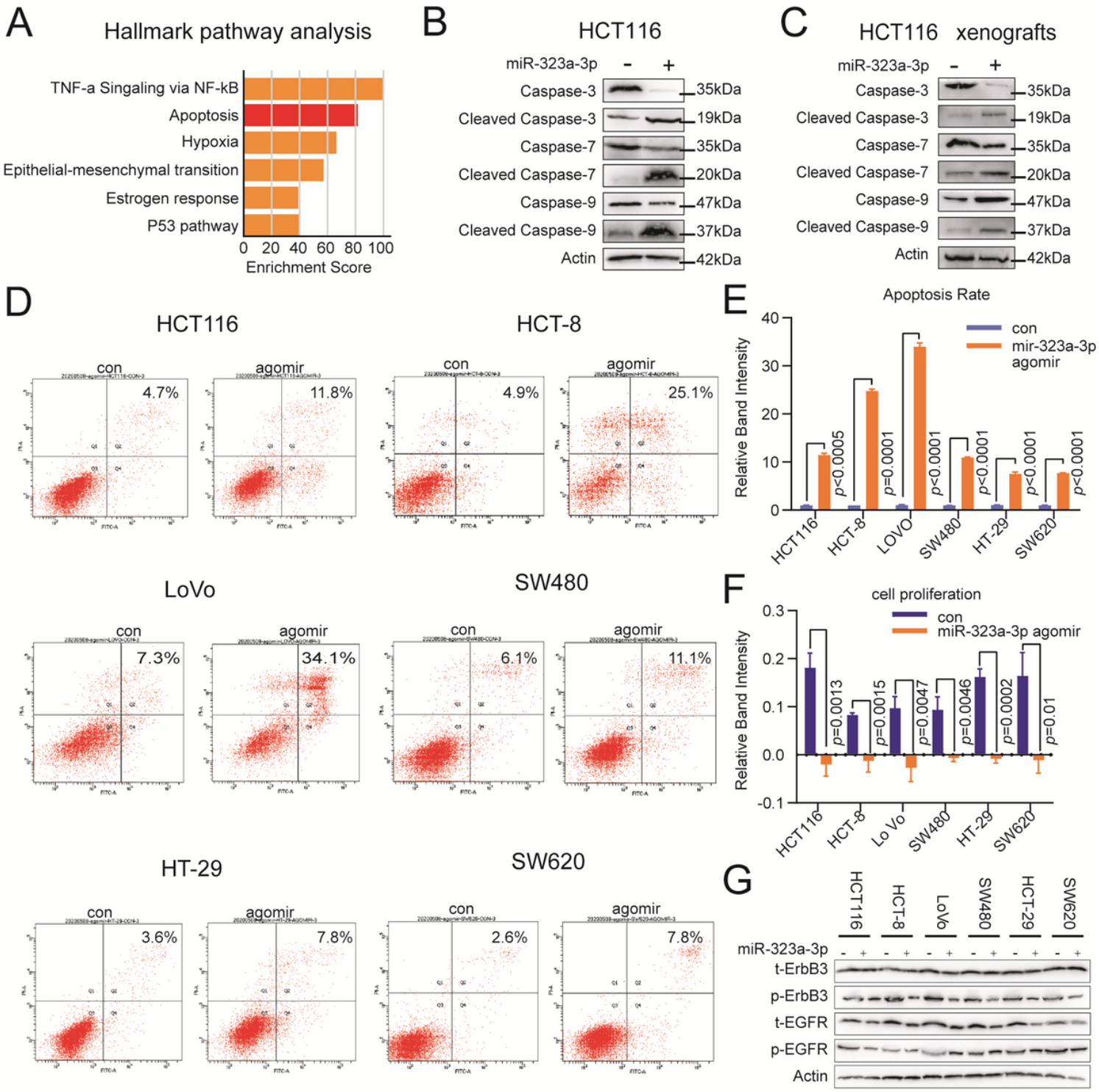

Figure 3

MiR-323a-3p inhibits tumor growth by promoting apoptosis in CRC in vitro and in vivo. A. Apoptosis is one of the primary processes that is altered in miR-323a-3p-overexpressing HCT116 cells as determined by hierarchical clustering analysis. Scale bar for expression levels is shown. B. Apoptotic protein markers were activated in agomir-treated HCT116 cells (n=3 per group). C. Apoptosis protein markers were activated in agomir-treated HCT116 xenograft tissues. D. Apoptosis rates were increased in CRC cells treated with agomir for 72 hr as shown by flow cytometry analysis (n=3 per group). E. Analysis of the

apoptosis rate . F. CRC cell proliferation was decreased in response to treatment with agomir and xCELLigence RTCA DP. G. Total and phosphorylated EGFR and ErbB3 protein levels were decreased in agomir-treated CRC cells (n=3 per group).

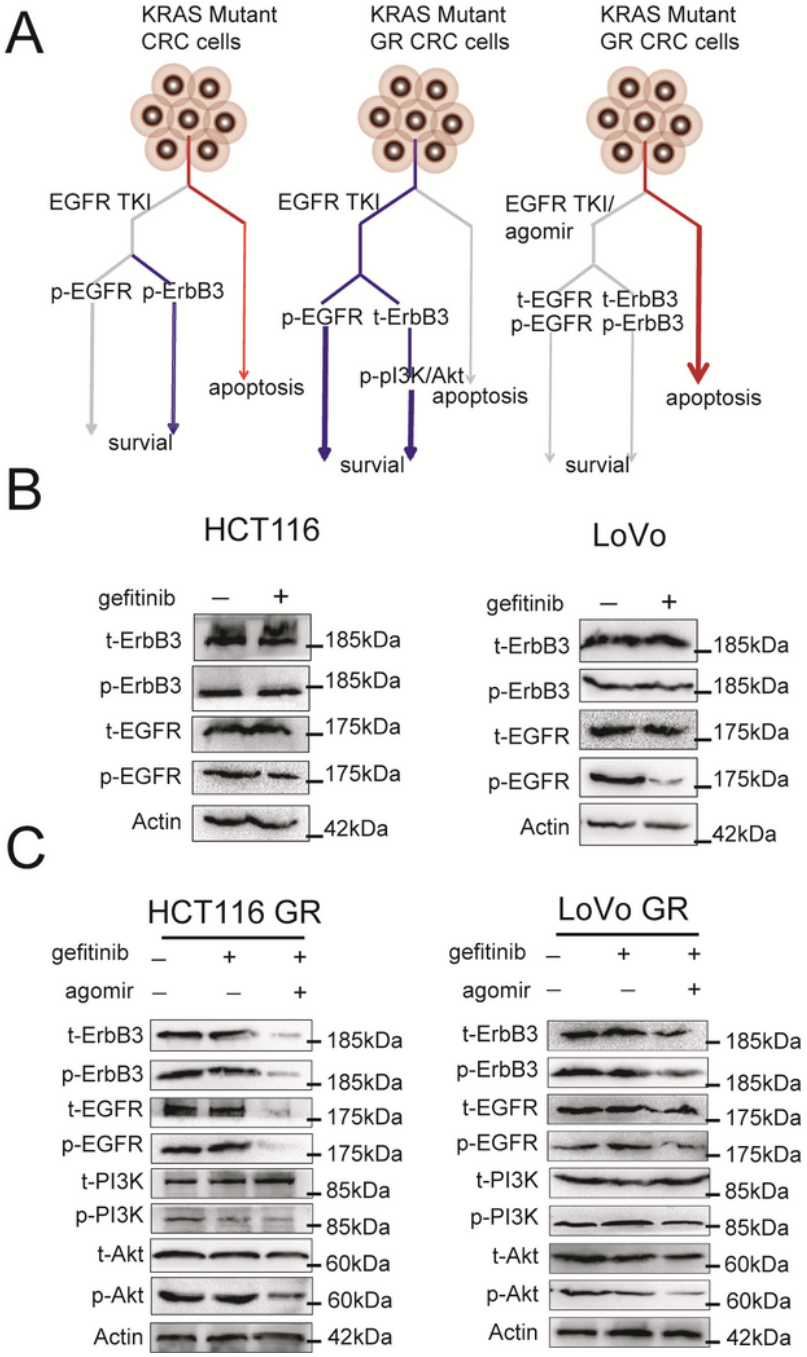

Figure 4

MiR-323a-3p inhibits EGFR/ErBB3 activation in GR KRAS mutant CRC cells. A. ErbB3 is highly expressed in KRAS mutant CRC tissues that escape EGFR-TKI inhibition. EGFR/ErbB3 is activated in KRAS mutant

GR CRC cells that escape gefitinib inhibition. MiR-323a-3p inhibits tumor growth of acquired GR KRAS mutant cell lines and ErbB3 high expression KRAS mutant CRC tissues by inhibiting expression of EGFR and ErbB3. B. Total and phosphorylated levels of EGFR and ErbB3 proteins were decreased in gefitinib-treated HCT116 and LoVo cells (n=3 per group). C. Phosphorylated EGFR, ErbB3, PI3K and Akt proteins in HCT116 GR and LoVo GR cells did not change after gefitinib administration, but they were significantly reduced after the addition of agomir (n=3 per group).

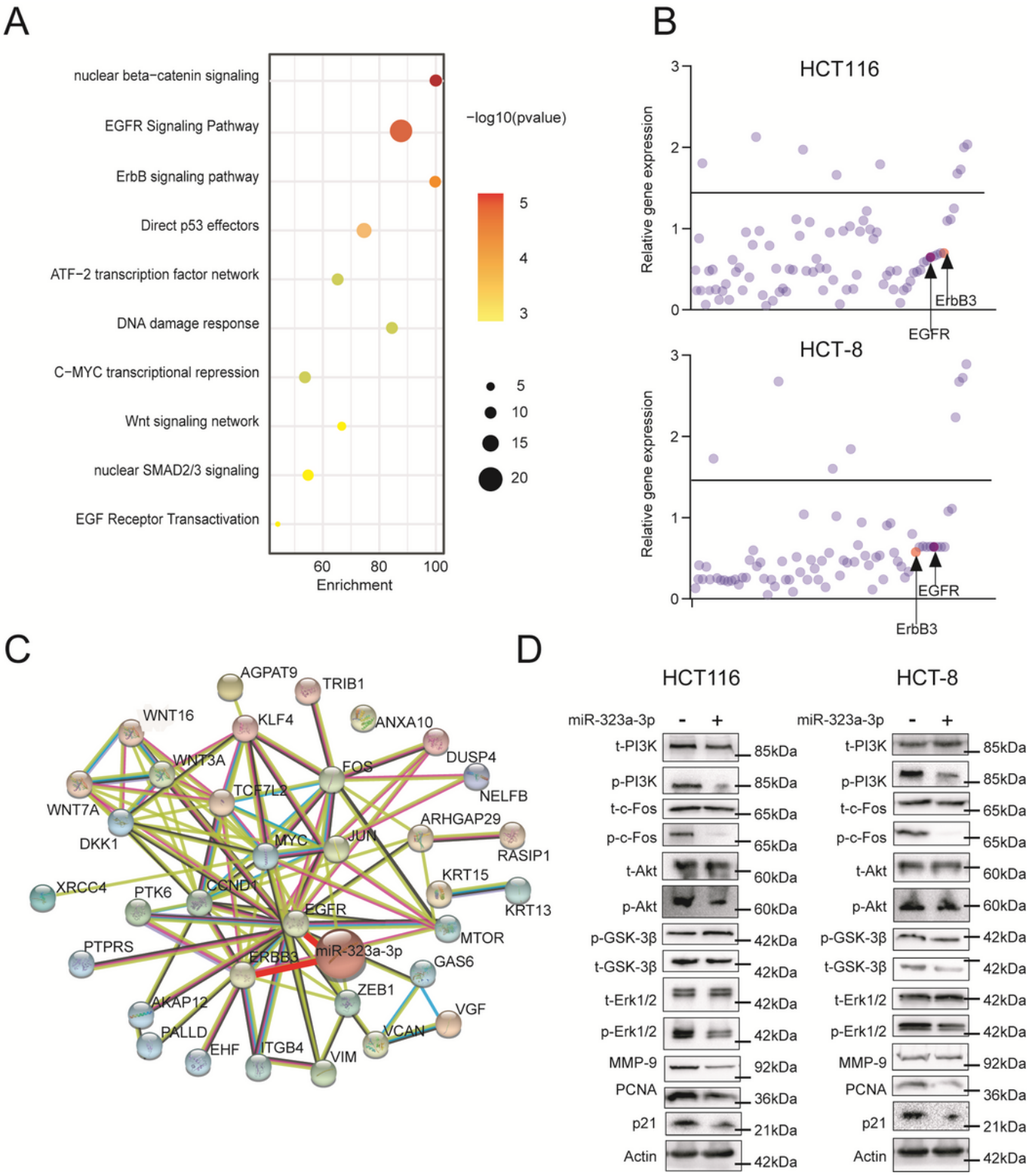

Figure 5

The molecular regulatory network of miR-323a-3p. A. Scatter plot of enriched KEGG pathways showing that EGFR and ErbB3 are prominent in the network. The enrichment factor is the ratio of the differentially expressed gene number to the total gene number in a certain pathway. The color and size of the dots represent the range of the p-value and the number of DEGs mapped to the indicated pathways, respectively. The top 10 enriched pathways are shown in the figure. B. Lentiviruses carrying control or miR-323a-3p were used to transduce HCT116 and HCT-8 cells, and expression of downregulated genes was determined by quantitative real-time reverse-transcription polymerase chain reaction (qRT-PCR) (n=3 per group). C. Functional enrichment of intersecting genes by web-STRING and a protein-protein interaction network. D. Levels of p-PI3K, p-c-fos, p-Akt, p-Gsk-3β, p-Erk1/2, MMP9, PCNA and p21 proteins in cell lysates of HCT116 and LoVo cells were significantly reduced in response to overexpression of miR-323a-3p (n=3 per group).

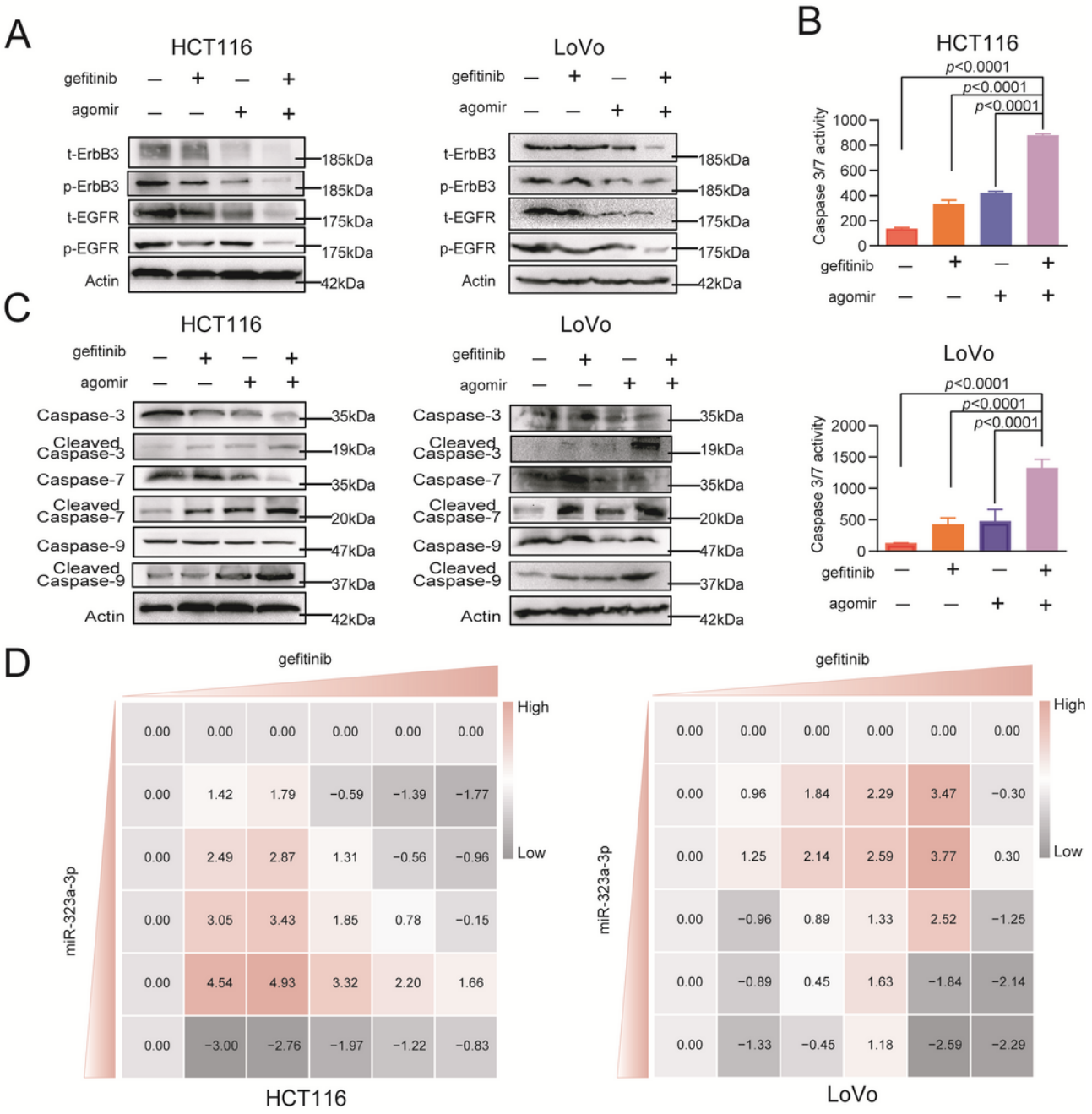

Figure 6

MiR-323a-3p and gefitinib synergistically inhibit CRC cell proliferation. A. Total and phosphorylated EGFR and ErbB3 decrease more significantly after gefitinib and agomir coadministration than after a single administration of either (n=3 per group). B. The combination of gefitinib and agomir elicited stronger caspase-3/7 activity than the single administration. C. Apoptotic protein markers were activated more significantly after gefitinib and agomir coadministration than after a single administration (n=3 per group). D. Heatmaps of Bliss synergy scores showing synergistic activities of miR-323a-3p and gefitinib in HCT116 cells (agomir: 0, 0.1, 0.3, 1, 3, 10, 30 nM; gefitinib: 0, 12.5, 25, 50, 100, 200, 400 nM) and LoV0

cells (agomir: 0, 0.25, 0.5, 1, 2, 4, 8 μM; gefitinib: 0, 1, 3, 10, 30, 100, 300 nM). The results showed that gefitinib and agomir had synergistic effects in the Bliss method.

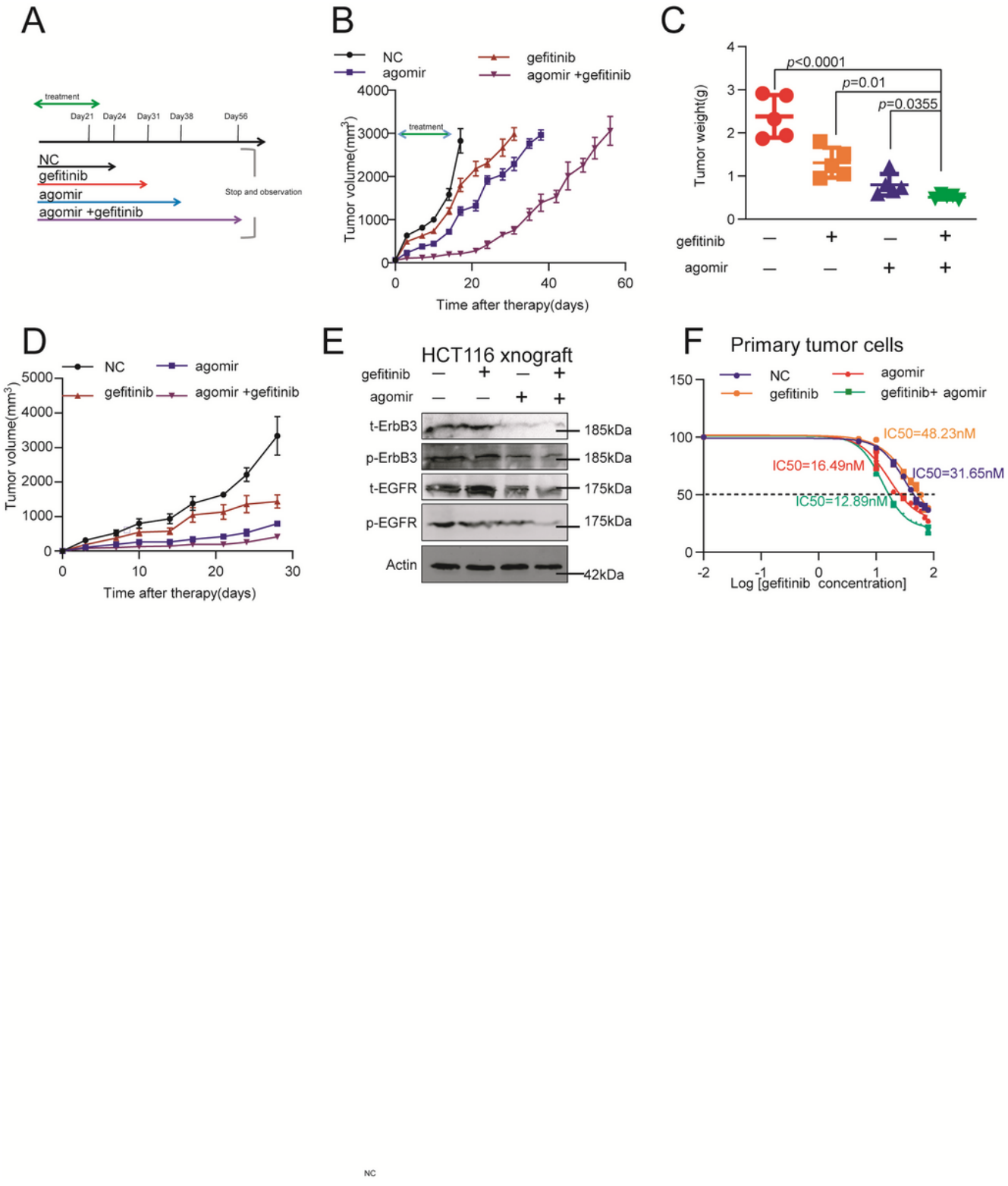

Figure 7

MiR-323a-3p and gefitinib synergistically inhibit tumor growth, and miR-323a-3p blocks acquired gefitinib resistance formation in a xenograft model. A. Schematic diagram of drug delivery model. B. Subcutaneous tumors grew more slowly and survived longer with the combination of gefitinib and

agomir than with single dosing of either agent. Mice with HCT116 cell line-derived xenograft tumors were treated with PBS (injected, n = 10 mice), gefitinib 25 mg/kg (oral gavage, n = 10 mice), agomir 5 nM per mouse (injected, n =10 mice), or gefitinib 25 mg/kg plus agomir 5 nM per mouse (n =10 mice) administered 3 times per week for an additional 21 days. Tumor volumes were measured over time from the start of treatment (mean ± sem.). p-values are provided (two-sided Student's t-tests). C. The weight of subcutaneous tumors decreased more significantly with the combination of gefitinib and agomir than with agomir alone. Tumor weight was measured when mice were euthanized (n=10 per group). Results are represented as the mean ± SEM. D. The volume of subcutaneous tumors decreased more significantly with the combination of gefitinib and agomir administration than with single administration. Tumor volume was measured twice per week. E. Protein levels of EGFR and ErbB3 in subcutaneous tumor tissue samples decreased more significantly after combined administration of gefitinib and agomir than after single administration. The data shown are representative of two independent experiments. F. The IC50 of gefitinib in tumor progenitor cells in the xenograft model was much lower in the coadministered group than in the single agent-administered group.

Supplementary Files

This is a list of supplementary files associated with this preprint. Click to download.

- Suplegends.pdf